Macromolecular Research

Review

DOI 10.1007/s13233-019-7053-0

www.springer.com/13233 pISSN 1598-5032 eISSN 2092-7673

Strategies to Improve Electrical and Electronic Properties of PEDOT:PSS for Organic and Perovskite Optoelectronic Devices

Su-Hun Jeong[†,1]
Soyeong Ahn[†,2]
Tae-Woo Lee[*,1,3,4]

[1] Department of Materials Science and Engineering, Seoul National University, 1 Gwanak-ro, Gwanak-gu, Seoul 08826, Korea
[2] Department of Materials Science and Engineering, Pohang University of Science and Technology (POSTECH), 77 Cheongam-Ro, Nam-Gu, Pohang, Gyeongbuk 37673, Korea
[3] BK21 PLUS SNU Materials Division for Educating Creative Global Leaders, Seoul National University, 1 Gwanak-ro, Gwanak-gu, Seoul 08826, Korea
[4] Nano Systems Institute (NSI), Institute of Engineering Research, Research Institute of Advanced Materials, Seoul National University, Gwanak-ro, Gwanak-gu, Seoul 08826, Korea

Received July 3, 2018 / Revised September 20, 2018 / Accepted September 24, 2018

Abstract: Poly(3,4-ethylenedioxythiophene):poly(styrenesulfonate) (PEDOT:PSS) is the most successful commercialized conducting polymer. PEDOT:PSS is a mixture of two ionomers: positively-charged PEDOT and negatively-charged PSS. PEDOT is a conducting polymer, which has π-π conjugation in its main backbone, and PSS increases charge carrier density in PEDOT by removing electrons from PEDOT during the synthesis process. Many researchers have tried to increase the electrical conductivity, k, of PEDOT:PSS films and applied them to organic and metal halide perovskite optoelectronic devices as transparent electrodes. Recently, the electrical properties of PEDOT:PSS, including k and work function, have been optimized for those optoelectronic devices. Here, we review recent strategies for optimizing the electrical properties of PEDOT:PSS to use them as transparent electrodes.

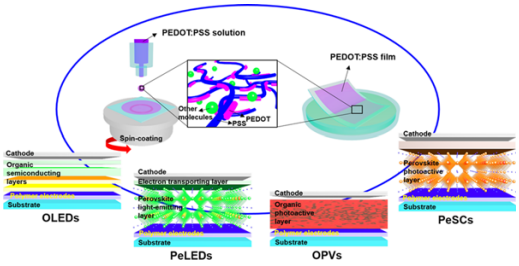

Keywords: PEDOT:PSS, transparent electrode, conductivity, work function, optoelectronic devices.

1. Introduction

Optoelectronic devices including light-emitting diodes and solar cells require at least one transparent electrode for light to penetrate. The most widely-used and commercially-successful transparent electrode material is indium tin oxide (ITO).[1] However, the brittle nature of ITO remains the biggest obstacle to its use in flexible optoelectronic devices. To replace it, flexible transparent materials have been developed, including conducting polymers,[2-7] silver nanowires,[8-10] carbon nanotubes,[11] and graphene.[12-16] Among them, conducting polymers have been widely investigated due to their easy solution-processability for thin films, high transmittance and amenability to tailoring of electrical conductivity.[6] Poly(3,4-ethylenedioxythiophene):poly(styrenesulfonate) (PEDOT:PSS) (Figure 1(a)) is the most successful conducting polymer. It has been commercialized and widely used for fundamental research on conducting polymers and their applications. PEDOT:PSS solutions are mainly provided from Heraeus Co. (Hanau, Germany), and the solutions vary depending on their uses (Clevios™ PH 500, PH 1000 for transparent electrodes and Clevios™ P VP AI4083 for buffer layers). PEDOT:PSS is a mixture of two ionomers: positively-charged PEDOT and negatively-charged PSS. PEDOT is a conducting polymer, which has π-π conjugation in its main backbone. PSS removes electrons from PEDOT and increases charge carrier density in PEDOT during the synthesis process. Also, the hydrophilic nature of PSS stabilizes PEDOT chains and disperses them in water in the form of particles.[17] Therefore, thin PEDOT:PSS films can be easily obtained by solution processes including spin-coating, bar-coating,[18] spray-coating,[19] and shear-coating.[5]

Many attempts have been made to obtain highly conductive PEDOT:PSS films and apply them as transparent electrodes for organic and metal halide perovskite optoelectronic devices.[3,4,12,20-26] For PEDOT:PSS to be used as electrodes, additional processes are required to increase its electrical conductivity k. These processes are divided into two main categories: i) use of additives and ii) post-treatment (Figure 1(b)). The additive method is to add polar organic solvents with high boiling points (*e.g.*, dimethyl sulfoxide (DMSO),[27,28] ethylene glycol (EG),[29] glycerol,[30] sorbitol[31]) to PEDOT:PSS aqueous solution. Incorporation of surfactants with

Acknowledgments: This research was supported by the Nano Material Technology Development Program through the National Research Foundation of Korea (NRF) funded by the Ministry of Science and ICT (NRF-2014M3A7B4051747). Also, this work was supported by the National Research Foundation of Korea (NRF) grant funded by the Korea government (Ministry of Science and ICT) (NRF-2016R1A3B1908431). This research was also supported by Creative Materials Discovery Program through the National Research Foundation of Korea (NRF) funded by Ministry of Science and ICT (2018M3D1A1058536).

***Corresponding Author:** Tae-Woo Lee (twlees@snu.ac.kr, taewlees@gmail.com)
[†]These authors equally contributed to this work.

polar organic solvents can improve both *k* and stretchability of PEDOT:PSS films.[20,21] The highest *k* of PEDOT:PSS (Clevios™ PH 1000) films made by the additive methods was achieved through the addition of 5 wt% DMSO, and the resultant *k* was 945 S/cm.[27]

Post-treatments are carried out after the formation of PEDOT:PSS films. The *k* of PEDOT:PSS films treated with organic polar solvents[5,22-24,32,33] or acid solvents[3,4] has been dramatically increased compared to that of the films with additives. Especially, the post-treatments with strong acids, including H_2SO_4 and HNO_3, increased the *k* above 4,000 S/cm. Recently, the post-treatment using a shear coating with methanol increased the *k* up to 4,600 S/cm for PEDOT:PSS (Clevios™ PH 1000).[5] Basically, these processes enhance the π-π stacking, which acts as current path, between conducting PEDOT chains by weakening the interaction between positively-charged PEDOT and negatively-charged PSS and removing excess amount of uncoupled insulating PSS chains from films. Besides increasing the *k* of PEDOT:PSS films, the importance of optimizing their work function (WF) has been highlighted to improve charge injection/extraction and device performance.[2,24,34,35]

We review the recent progress on improving the electrical properties of PEDOT:PSS electrodes, including *k* and WF, and also review their applications to organic and perovskite optoelectronic devices as transparent electrodes (Figure 1(c)).

2. Recent strategies to improve electrical properties of PEDOT:PSS electrodes for optoelectronic devices

In this review, we introduce recent strategies that boost PEDOT:PSS electrodes towards manufacturing high-performance organic and metal halide perovskite optoelectronic devices. Significant enhancement in electrical properties of PEDOT:PSS, including *k* and WF, has been achieved using diverse approaches. Recent easy approaches to PEDOT:PSS electrodes and their application to optoelectronic devices are reviewed here.

2.1. Strategies to improve *k* of PEDO:PSS electrodes

2.1.1. Strong acid-based post-treatment

Additive methods have increased the *k* of PEDOT:PSS (Clevios™ PH 1000) up to 945 S/cm by adding 5 wt% DMSO.[27] However, insulating PSS remained at the surface of PEDOT:PSS films and limited the increase in *k*. Many post-treatment methods have been developed to increase the *k* of PEDOT:PSS by removing insulating PSS uncoupled with PEDOT on the surface of PEDOT:PSS films.[22-24,32,36-38] These post-treatment methods used various organic polar solvents: EG,[22,32,36] hexafluoroacetone (HFA)[24] methanol,[33] and glycol monostearate.[23] EG-based post-treatment increased the *k* of PEDOT:PSS (Clevios™ PH 1000) films to 1,418 S/cm and achieved practical use in small-molecule organic photovoltaics (OPVs).[22] HFA-based post-treatment attained *k*=1,019 S/cm.[23]

Recently, Kim *et al*. increased the *k* of PEDOT:PSS (Clevios™ PH 1000) films up to 4,380 S/cm by employing H_2SO_4 post-treatment method.[4,37] Highly-concentrated H_2SO_4 separates into $H_3SO_4^+$ and HSO_4^-. During the post-treatment in which PEDOT:PSS films were immersed in H_2SO_4 solvent, these two ions stabilize the isolated state of two charged polymers, positively-charged PEDOT and negatively-charged PSS. (Figure 2(a)), to yield PEDOT-rich and PSS-rich domains. Subsequently, washing the films with water removed only hydrophilic PSS that was not coupled with PEDOT. Absorption spectra proved the removal of PSS by the H_2SO_4 post-treatment (Figure 2(b)). The H_2SO_4 post-treatment significantly reduced absorption in the UV range, but did not affect absorption in the visible or IR regions. Since Phenyl moieties in PSS absorb UV light, and the free charge carriers in PEDOT

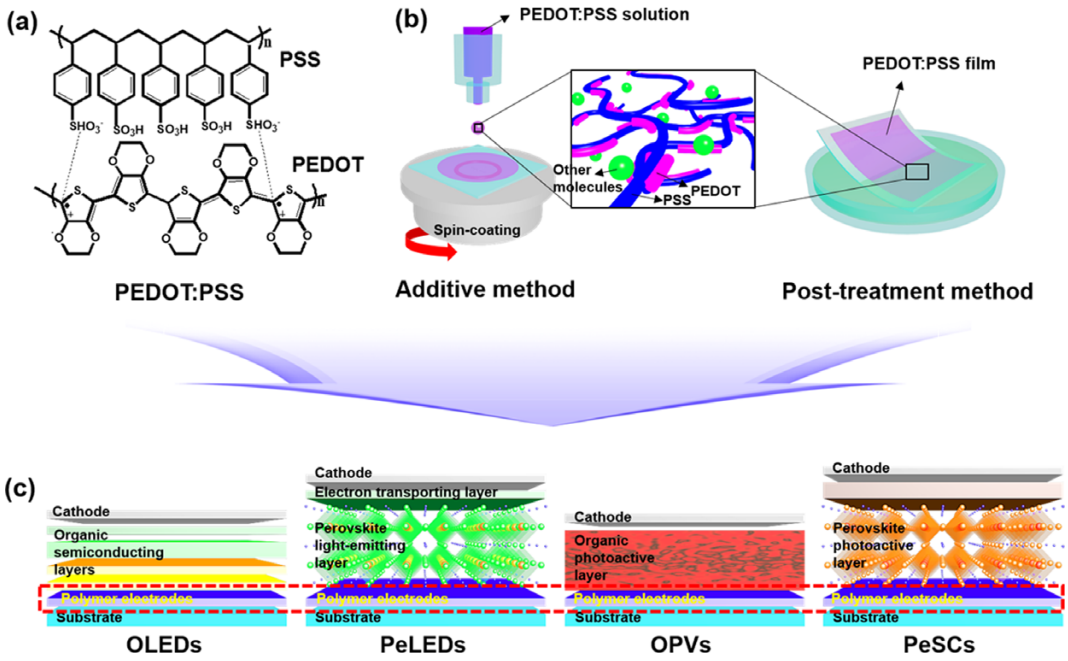

Figure 1. (a) Chemical structure of PEDOT:PSS. Schematic illustrations of (b) methods to improve the electrical properties of PEDOT:PSS electrodes and (c) their applications to organic and metal halide perovskite optoelectronic devices, including organic light-emitting diodes (OLEDs), perovskite light-emitting diodes (PeLEDs), organic photovoltaics (OPVs), and perovskite solar cells (PeSCs).

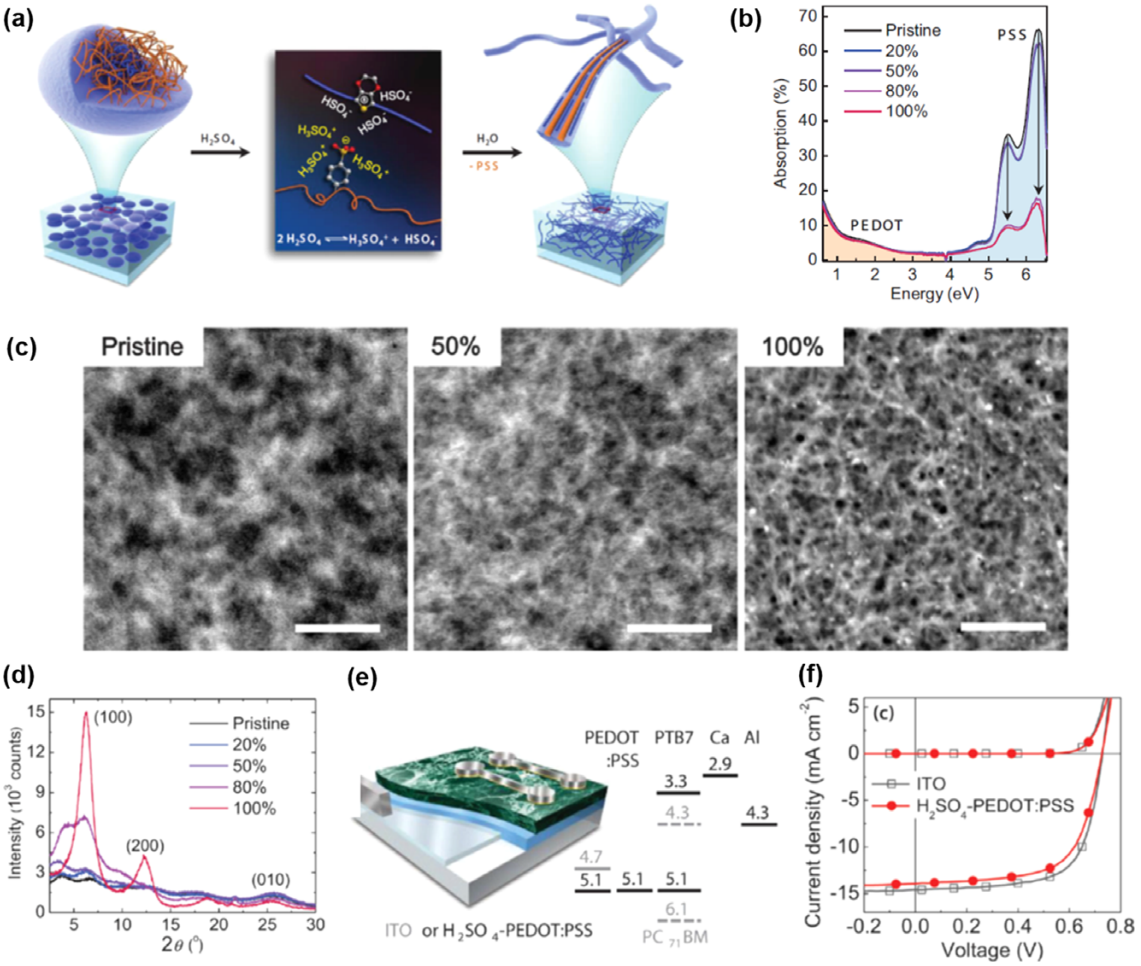

Figure 2. (a) Schematics of H_2SO_4 post-treatment. (b) Absorption spectra, (c) HAADDF-STEM images (Scale bars, 200 nm), and (d) XRD spectrum of PEDOT:PSS films treated by H_2SO_4 solutions with varying concentrations. Application of H_2SO_4-treated PEDOT:PSS electrodes to (e) OPVs. (f) *J-V* characteristics of OPVs on top of H_2SO_4-treated PEDOT:PSS and ITO/PEDOT:PSS electrodes: Reproduced with permission from Ref. 3, N. Kim *et al.*, *Adv. Mater.*, **26**, 2268 (2014). © 2014, WILEY-VCH Verlag GmbH & Co. KGaA, Weinheim.

absorb visible and IR light, these results demonstrate that the treatment selectively removed the insulating PSS, but not the conducting PEDOT.

Besides the removal of insulating PSS chains, the H_2SO_4 post-treatment also induced restructuring in PEDOT:PSS films. A high-angle annular dark-field scanning transmission electron microscope (HAADF-STEM) revealed that the surface morphologies changed from a granular structure to a nanofibril structure as the concentration of H_2SO_4 solution increased (Figure 2(c)). The nanofibril structure was attributed to the π-π staking nature and the rigidity of thiophene rings in PEDOT backbone. The X-ray diffraction (XRD) patterns also revealed well-connected PEDOT chains and improved π-π stacking of PEDOT chains after the treatment (Figure 2(d)). XRD peaks were detected at 2θ=3.8° and 6.6°; they correspond to the lamellar stacking of two distinct orderings of PEDOT and PSS, respectively. After the H_2SO_4 post-treatment, the intensities of peaks at 2θ=3.8° and 6.6° were significantly increased; this change means that the crystallinity improved in the PEDOT:PSS films. The H_2SO_4 post-treatment induced organization of PEDOT chains into well-connected and well-crystallized networks, which facilitated efficient intra- and inter- chain charge transport and achieved *k* up to 4,380 S/cm.

The *k*-increased PEDOT:PSS films were used as transparent electrodes of OPVs, and, for a comparative study, a device was fabricated on the conventional ITO/PEDOT:PSS (Clevios™ P VP AI4083) buffer layer (Figure 2(e)). The OPVs on the H_2SO_4-treated PEDOT:PSS and ITO/PEDOT:PSS had very similar current density-voltage (*J-V*) characteristics (Figure 2(f)), and both had power conversion efficiencies (PCEs) of 6.6%. The H_2SO_4-treated PEDOT:PSS films also can be transferred onto arbitrary substrates, including plastic substrates.[4] Therefore, this method can facilitate versatile integration of films with any substrates and with organic/inorganic semiconducting materials to fabricate various flexible optoelectronic devices. However, post-treatment with strong acid is too dangerous to be suitable in industry. Also, the film is too thin (~50 nm) after the H_2SO_4 post-treatment and the sheet resistance is still too high to be practical for large-scale optoelectronic devices (46.1 Ω/□).

Besides the H_2SO_4-treated, HNO_3-treatment increased the *k* of PEDOT:PSS (Clevios™ PH 1000) up to 4,100 S/cm.[39,40] The treatment was achieved by dropping the 14 M HNO_3 solution on the PEDOT:PSS films at room temperature and blowing N_2 gas. The increase in HNO_3 concentration increased in *k* (1,810 S/cm for 3 M HNO_3). The treatment induced phase separation

of PEDOT:PSS and selectively removed the PSS domains, resulting in highly enhanced inter-chain coupling of PEDOT. The treatment decreased the thickness from ~100 nm to ~30 nm. ITO-free semi-transparent perovskite photovoltaics (PeSCs) were fabricated by employing the HNO_3-treated PEDOT:PSS films as both anode and cathode, exhibiting 13.9% of PCE.[40] The ITO-free tandem solar cell stacking silicon-based solar cell on PeSCs showed high PCE of 19.2%.

2.1.2. Preferential alignment of conducting PEDOT

Phase separation of PEDOT and PSS chains and preferential alignment of PEDOT chains can increase the *k* of PEDOT:PSS (Clevios™ PH 1000) films to 4,600 S/cm even without strong acid-based treatments.[5] B. J. Workfolk *et al*. used the solution-shearing method (Figure 3(a)) which can yield highly-conductive PEDOT:PSS films with preferentially aligned and ordered PEDOT chains. Solution-shearing methods have been usually used to achieve molecular packing and ordering of organic conjugated materials.[41] The solution-shearing method uses a top shearing plate, which entails dragging the solution across a substrate and keeping the bulk of the solution between the top plate and the substrate.[42] Appropriate control of the temperature of the substrate and the shearing speed of the top plate provides sufficient time for conjugated materials to become aligned and ordered. The solution-shearing was used both to align the conjugated PEDOT chains during the PEDOT:PSS thin film fabrication and to remove surface-enriched insulating PSS by using methanol.[41]

Compared to the spin-cast films, the sheared films showed well-defined elongated nanofibers (Figure 3(c)). These fiber networks were well interconnected, so charge transport occurred efficiently. To determine why shear coating achieved the high *k*, depth profiles were measured using X-ray photoelectron spectroscopy (XPS). These profiles showed different gradient compositions in the depth direction, depending on whether the films were deposited by spin coating or shear coating (Figure 3(c)). Compared to the spin-coated films, the sheared films showed a larger extent of phase separation of PSS- and PEDOT-rich regions.

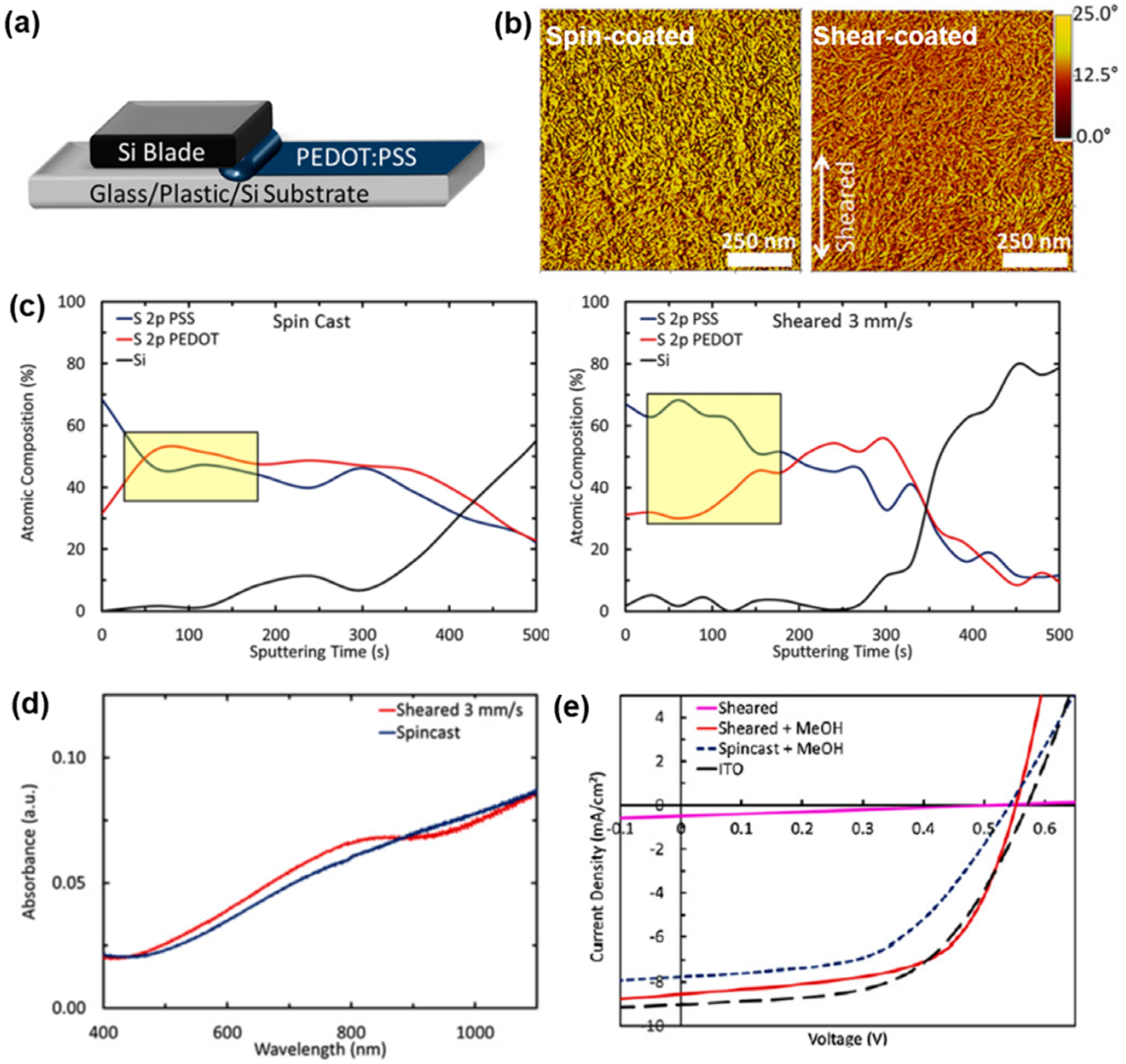

Figure 3. (a) Schematic of shearing-coating method. (b) Atomic force microscopy (AFM) images and (c) XPS depth profiles of spin-cased and solution-sheared PEDOT:PSS films. (d) Unpolarized absorption in spin-cast and sheared PEDOT:PSS films. (e) *J-V* characteristics of OPVs on various anodes including PEDOT:PSS (spin-cast and solution-sheared) and ITO. Reproduced with permission from Ref. 5, B. J. Workfolk *et al*., *PNAS*, **112**, 14138 (2015). © 2015, National Academy of Sciences.

This increase in separation means that larger amounts of surface-enriched hydrophilic PSS on sheared films can be easily removed during solution-shearing of methanol than during spin coating. Polarized absorption spectroscopy revealed the removal of more PSS from the sheared films than from the spin-coated films. In the non-polarized absorption (Figure 3(d)), the sheared films showed weak and broad absorption near 800 nm, which suggests that a highly conductive phase existed in the sheared films, and that the insulating PSS was better removed than in the spin-coated films.

The sheared PEDOT:PSS film with high k was applied as transparent anodes in OPVs. The OPV on the sheared film showed a PCE=2.87%, which was comparable to that of the OPV on ITO (2.86%). Especially, the device on sheared film obtained higher fill factors than that of the device on ITO; this improvement can be attributed to the high k of the sheared PEDOT:PSS film and to possible improvement of the morphology of a photoactive layer by the supporting film. The solution-shearing method is promising due to its compatibility with a roll-to-roll printing process for continuous mass production.

2.1.3. Purification of PEDOT:PSS solution

Recently, the effect of the purity of the PEDOT:PSS solution on k of the film has been emphasized. The final PEDOT:PSS solution after synthesis includes impurities, such as uncoupled PSS, residual oxidants, 3,4-ethylenedioxythiophene oligomers, and residual electrolytes, which inhibit charge transport. Purification by ultrafiltration can yield highly-conductive, air-stable PEDOT:PSS.[43] The process (Figure 4(a)) uses an ultrafiltration cell that has membrane pore size=100 nm, which is larger than the impurities and smaller than the PEDOT:PSS particles. As the number of purification passes increased, the k of PEDOT:PSS films increased to 2,000 S/cm (Figure 4(b)). This high k was achieved by adding only 5 wt% DMSO, and did not require post-treatment.

The increased k can be explained by the removal of uncoupled PSS during the purification process. The removal of PSS was confirmed by XPS (Figure 4(c)) and absorption (Figure 4(d)) results. In the S 2p XPS spectra of PEDOT:PSS films, the peak between 166 and 170 eV corresponds to the binding energy of the sulfur atoms in PSS, and the peak between 162 and 166 eV corresponds to the binding energy of the sulfur atoms in PEDOT.[44] Therefore, the change in the ratio of PEDOT to PSS after purification can be identified by the S 2p XPS spectrum. After the fifth purification pass, the ratio of peak intensities for PEDOT to PSS increased; this change implies that uncoupled PSS was removed (Figure 4(c)). Also, the purification caused conversion of sulfonate residues to sulfonic acid, and thereby increased the energy level of the S 2p XPS peak of sulfur atoms in PSS. This result means that the converted sulfonic acid formed additional doped states between PEDOT and PSS. In the absorption spectrum (Figure 4(d)), the absorption band in the UV was significantly decreased after the purification; this change indicates that PSS had been removed. A red shift in the peaks in the Raman spectrum confirmed the removal of PSS (Figure 4(e)).

The purified PEDOT:PSS film was more stable than the pristine film. Sheet resistance (R_S) (Figure 4(f)) of pristine and purified PEDOT:PSS films depended on the storage time in ambient air. After 1 week, R_S of pristine PEDOT:PSS film increased from 151.3 Ω/□ to 185.6 Ω/□, but R_S of the purified PEDOT:PSS

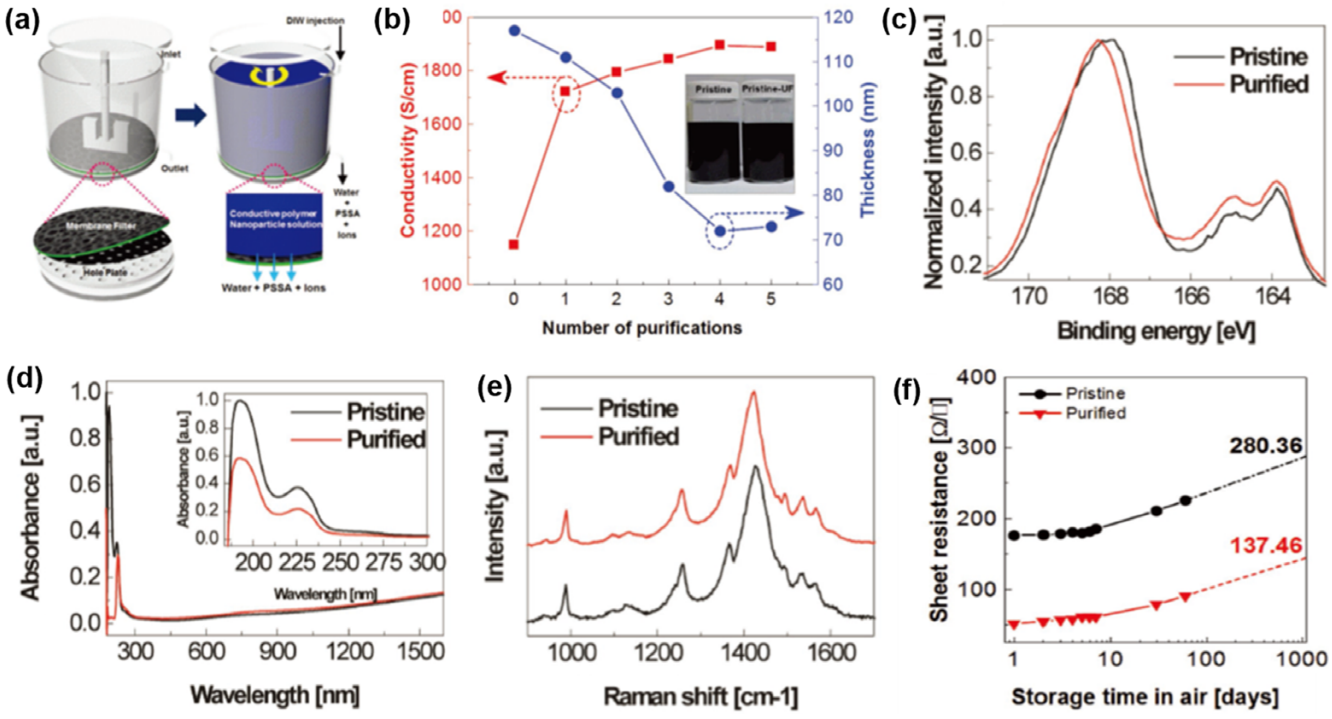

Figure 4. (a) Schematics of purification of PEDOT:PSS solutions by using an ultrafiltration cell. (b) Conductivity of PEDOT:PSS films *vs.* number of purification passes. (c) XPS, (d) absorption, (e) Raman spectrum, and (f) sheet resistance stability of PEDOT:PSS films fabricated using the pristine and purified solutions. Reproduced with permission from Ref. 43, S. Kim *et al.*, *Adv. Mater.*, **28**, 10149 (2016). © 2016, WILEY-VCH Verlag GmbH & Co. KGaA, Weinheim.

Table 1. Summary of recent progress on electrical properties of PEDOT:PSS films

PEDOT:PSS type	Method	Thickness (nm)	Sheet resistance (Ω/□)	Conductivity (S/cm)	Work function (eV)	Ref.
Clevios™ PH 1000	Post-treatment with H_2SO_4	-	46.1	4,380	-	3
Clevios™ PH 1000	Post-treatment with HNO_3	30	11	4,100	-	39
Clevios™ PH 1000	Post-treatment using the shear-coating with methanol	-	17±1	4,600±100	-	5
Synthesized	Ultrafiltration & DMSO additive	36	37.8±4.5	2,000	4.87	43
Clevios™ PH 500	PFSA & DMSO additives	100	2,000	50	5.80	2

film increased only from 151.3 Ω/□ to 156.5 Ω/□. The extrapolated R_S was much lower in purified PEDOT:PSS film than in pristine film. Therefore, purification of PEDOT:PSS solution can improve both *k* and stability of PEDOT:PSS films.

2.2. Strategies to improve WF of PEDOT:PSS electrodes

WF is another significant parameter that is used to evaluate transparent electrodes for optoelectronic devices. Removing PSS from the surface of PEDOT:PSS films reduced its surface WF,[45,46] in addition to increasing its *k*. As *k* increased, the resultant surface WF of PEDOT:PSS films (Clevios™ PH 1000) decreased to 4.8-5.0 eV.[35,43,47,48] Therefore, when highly-conductive PEDOT:PSS films were used as transparent anodes for optoelectronic devices, additional buffer layers were required to establish Ohmic contact with overlying semiconducting layers and to improve hole injection/extraction.[12,22,24,37]

Adding a perfluorinated ionomer, tetrafluoroethylene-perfluoro-3,6-dioxa-4-methyl-7-octenesulphonic acid copolymer (PFSA) to PEDOT:PSS solution with 5 wt% DMSO increases the surface WF of PEDOT:PSS-based polymeric anodes (called as "AnoHIL").[2,34] As the amount of added PFSA increased, the surface WF increased to 5.8 eV. PFSA has high ionization potential due to its fluorocarbon chains. Especially, its lower surface energy (~20 mN m^{-1}) than that of PSS (~71-73 mN m^{-1}) causes PFSA to become surface-enriched in the anode films (Figure 5(a)). The XPS depth profile results confirmed that PFSA self-organized toward the film surface (Figure 5(b)). Dark injection space-charge limited current (DI-SCLC) measurement revealed that the high WF polymeric anodes (AnoHIL) can make Ohmic contact with the overlying semi-conducting layer without any buffer layer. The calculated hole injection efficiency of high-WF polymeric anodes was ~1 (Figure 5(c)), which is characteristic of Ohmic contact.

The high-WF polymer anodes increased the current efficiencies (CEs) of green phosphorescent organic light-emitting diodes (OLEDs) to 128 cd/A in single-cell devices and to 235 cd/A in tandem-cell device, which were much higher than those of conventional OLEDs on top of ITO anodes (88 cd/A in single-cell, 167 cd/A tandem cell) (Figure 5(d)). These high CEs were meaningful in that they were achieved even in simplified structures that lacked a hole injection layer (HIL). The high WF polymeric anodes showed a similar effect on the CE of metal halide perovskite light-emitting diodes (PeLEDs). The highest CE of PeLEDs on high WF polymeric anodes was 42 cd/A as the WF of anodes increased. The metal halide perovskite emitting material was green-emissive methyl ammonium lead bromide ($MAPbBr_3$). Its conduction band maxima (CBM) is about 5.89 eV,[34,49] which is much deeper than highest occupied molecular orbitals of conventional organic semiconducting mateirials.[6] However, the high

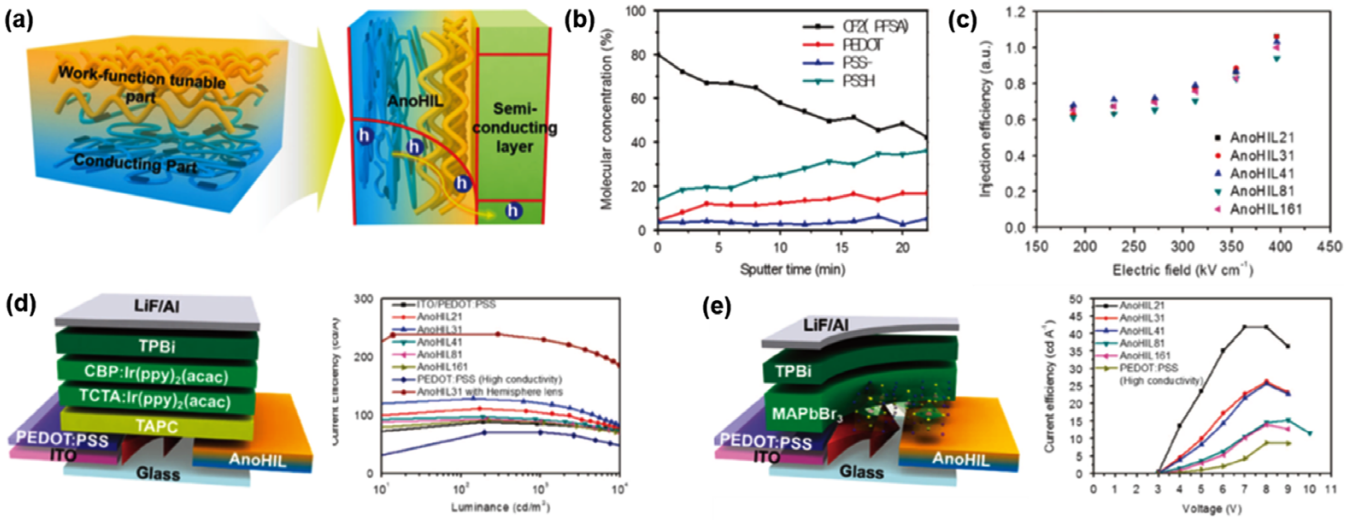

Figure 5. (a) Schematics of efficiency hole injection by the high WF polymeric anode. (b) Molecular depth profile of the high-WF polymeric anode film. (c) Improved hole injection from the high WF polymeric anode to the overlying organic semi-conducting layer. (d) Simplified OLEDs by high WF polymeric anodes and their current efficiencies. (e) Simplified PeLEDs by high WF polymeric anodes and their current efficiencies. Reproduced with permission from Ref. 2, S.-H. Jeong *et al.*, *NPG Asia Mater.*, **9**, e411 (2017). © 2017, Macmillan Publishers Limited, part of Springer Nature.

WF of polymeric anodes (~5.8 eV) was enough to make Ohmic contact with the CBM of the perovskite emitter without use of a HIL. As the WF of anodes increased, the turn-on voltages of devices decreased; this change means a reduction in the hole injection barrier from anodes to $MAPbBr_3$ layers. These results demonstrate the importance of optimizing the WF of PEDOT:PSS electrodes to improve device efficiency and to simplify device structure. We have summarized the *k* and WF of PEDOT:PSS electrodes treated with the previously introduced methods.

3. Conclusion and outlook

We have reviewed recent strategies to optimize the electrical properties of PEDOT:PSS electrodes for organic and metal halide perovskite optoelectronic devices; the methods include new post-treatments, purification and WF-tuning. Post-treatment using strong acid, and a process called shear-coating dramatically increased *k* to > 4,000 S/cm. Purification using ultrafiltration eliminated impurities from the PEDOT:PSS solution. Furthermore, incorporating an ionomer with high ionization potential energy into PEDOT:PSS effectively tuned the surface WF of PEDOT:PSS films up to 5.8 eV, and this high WF anodes significantly improved the *CEs* of OLEDs and PeLEDs, simplifying device structures. This applicability in both types of device implies that these WF methods are universal applicability to various optoelectronic devices. These approaches from various perspectives suggest methods to promote commercialization of PEDOT:PSS electrodes which are used for flexible optoelectronic devices. Chemical post-treatments to increase the *k* of PEDOT:PSS films are still not suitable for mass production fabricating large-area films. Also, the trade-off between *k* and WF of PEDOT:PSS films has been still challenging. However, we believe that further research on large-scale fabrication of optimized high-*k* PEDOT:PSS films with high WF will advance the possibility of commercializing printed flexible optoelectronic devices.

References

(1) A. Kumar and C. Zhou, *ACS Nano*, **4**, 11 (2010).
(2) S.-H. Jeong, S.-H. Woo, T.-H. Han, M.-H. Park, H. Cho, Y.-H. Kim, H. Cho, H. Kim, S. Yoo, and T.-W. Lee, *NPG Asia Mater.*, **9**, e411 (2017).
(3) N. Kim, S. Kee, S. H. Lee, B. H. Lee, Y. H. Kahng, Y. R. Jo, B.-J. Kim, and K. Lee, *Adv. Mater.*, **26**, 2268 (2014).
(4) N. Kim, H. Kang, J.-H. Lee, S. Kee, S. H. Lee, and K. Lee, *Adv. Mater.*, **27**, 2317 (2015).
(5) B. J. Worfolk, S. C. Andrews, S. Park, J. Reinspach, N. Liu, M. F. Toney, S. C. B. Mannsfeld, and Z. Bao, *Proc. Natl. Acad. Sci. U.S.A.* **112**, 14138 (2015).
(6) S. Ahn, S.-H. Jeong, T.-H. Han, and T.-W. Lee, *Adv. Opt. Mater.*, **5**, 1600512 (2017).
(7) H. Shi, C. Liu, Q. Jiang, and J. Xu, *Adv. Electron. Mater.*, **1**, 150017 (2015).
(8) W. Gaynor, S. Hofmann, M. G. Christoforo, C. Sachse, S. Mehra, A. Salleo, M. D. Mcgehee, M. C. Gather, B. Lüssem, L. Müller-meskamp, P. Peumans, and K. Leo, *Adv. Mater.*, **25**, 4006 (2013).
(9) S. J. Lee, Y.-H. Kim, J. K. Kim, H. Baik, J. H. Park, J. Lee, J. Nam, J. H. Park, T. Lee, G.-R. Yi, and J. H. Cho, *Nanoscale*, **6**, 11828 (2014).
(10) S. G. R. Bade, J. Li, X. Shan, Y. Ling, Y. Tian, T. Dilbeck, T. Besara, T. Geske, H. Gao, B. Ma, K. Hanson, T. Siegrist, C. Xu, and Z. Yu, *ACS Nano*, **10**, 1795 (2016).
(11) J. Wu, M. Agrawal, A. Becerril, Z. Bao, Z. Liu, Ý. Y. Chen, and P. Peumans, *ACS Nano*, **4**, 43 (2010).
(12) M. Cai, Z. Ye, T. Xiao, R. Liu, Y. Chen, R. W. Mayer, R. Biswas, K. Ho, R. Shinar, and J. Shinar, *Adv. Mater.*, **24**, 4337 (2012).
(13) T.-H. Han, M.-H. Park, S.-J. Kwon, S. Bae, H. Seo, H. Cho, J. Ahn, and T.-W. Lee, *NPG Asia Mater.*, **8**, e303 (2016).
(14) T. Han, S. Kwon, N. Li, H. Seo, W. Xu, K. S. Kim, and T. Lee, *Angew. Chem. Int. Ed.*, **798**, 6197 (2016).
(15) H.-K. Seo, H. Kim, J. Lee, M.-H. Park, S.-H. Jeong, Y.-H. Kim, S.-J. Kwon, T.-H. Han, S. Yoo, and T.-W. Lee, *Adv. Mater.*, **29**, 1605587 (2017).
(16) T.-H. Han, H. Kim, S.-J. Kwon, and T.-W. Lee, *Mater. Sci. Eng. R*, **118**, 1 (2017).
(17) J. Rivnay, S. Inal, B. A. Collins, M. Sessolo, E. Stavrinidou, X. Strakosas, C. Tassone, D. M. Delongchamp, and G. G. Malliaras, *Nat. Commun.*, **7**, 11287 (2016).
(18) S. Kim, S. Y. Kim, M. H. Chung, J. Kim, and J. H. Kim, *J. Mater. Chem. C*, **3**, 5859 (2015).
(19) J. G. Tait, B. J. Worfolk, S. A. Maloney, T. C. Hauger, A. L. Elias, J. M. Buriak, and K. D. Harris, *Sol. Energy Mater. Sol. Cells*, **110**, 98 (2013).
(20) D. J. Lipomi, J. A. Lee, M. Vosgueritchian, B. C. Tee, J. A. Bolander, and Z. Bao, *Chem. Mater.*, **24**, 373 (2012).
(21) M. Vosgueritchian, D. J. Lipomi, and Z. Bao, *Adv. Funct. Mater.*, **22**, 421 (2012).
(22) Y. H. Kim, C. Sachse, M. L. Machala, C. May, L. Müller-meskamp, and K. Leo, *Adv. Funct. Mater.*, **21**, 1076 (2011).
(23) W. Zhang, B. Zhao, Z. He, X. Zhao, H. Wang, S. Yang, H. Wu, and Y. Cao, *Energy Environ. Sci.*, **6**, 1956 (2013).
(24) Y. Xia, K. Sun, and J. Ouyang, *Energy Environ. Sci.*, **5**, 5325 (2012).
(25) Z. Yu, Y. Xia, D. Du, and J. Ouyang, *ACS Appl. Mater. Interfaces*, **8**, 11629 (2016).
(26) Y. Xia, K. Sun, and J. Ouyang, *J. Mater. Chem. A*, **3**, 15897 (2015).
(27) B. Zhang, J. Sun, H. E. Katz, F. Fang, and R. L. Opila, *ACS Appl. Mater. Interfaces*, **2**, 3170 (2010).
(28) I. Lee, G. W. Kim, M. Yang, and T. Kim, *ACS Appl. Mater. Interfaces*, **8**, 302 (2016).
(29) H. Yan, T. Jo, and H. Okuzaki, *Polym. J.*, **41**, 1028 (2009).
(30) M. W. Lee, M. Y. Lee, J. C. Choi, J. S. Park, and C. K. Song, *Org. Electron.*, **11**, 854 (2010).
(31) A. M. Nardes, M. Kemerink, M. M. De Kok, E. Vinken, K. Maturova, and R. A. J. Janssen, *Org. Electron.*, **9**, 727 (2008).
(32) N. Kim, B. H. Lee, D. Choi, G. Kim, H. Kim, J. Kim, J. Lee, Y. H. Kahng, and K. Lee, *Phys. Rev. Lett.*, **109**, 106405 (2012).
(33) D. Alemu, H.-Y. Wei, K.-C. Hod, and C.-W. Chu, *Energy Environ. Sci.*, **5**, 9662 (2012).
(34) H. Cho, S.-H. Jeong, M.-H. Park, Y.-H. Kim, C. Wolf, C.-L. Lee, J. H. Heo, A. Sadhanala, N. Myoung, S. Yoo, S. H. Im, R. H. Friend, and T.-W. Lee, *Science*, **350**, 1222 (2015).
(35) Y. Zhou, C. Fuentes-hernandez, J. Shim, J. Meyer, A. J. Giordano, H. Li, P. Winget, T. Papadopoulos, H. Cheun, J. Kim, M. Fenoll, A. Dindar, W. Haske, E. Najafabadi, T. M. Khan, H. Sojoudi, S. Barlow, S. Graham, J.-L. Brédas, S. R. Marder, A. Kahn, and B. Kippelen, *Science*, **336**, 327 (2012).
(36) C. M. Palumbiny, C. Heller, C. J. Scha, V. Ko, G. Santoro, S. V. Roth, and P. Mu, *J. Phys. Chem. C*, **118**, 13598 (2014).
(37) N. Kim, S. Kee, S. H. Lee, B. H. Lee, Y. H. Kahng, Y. R. Jo, B. J. Kim, and K. Lee, *Adv. Mater.*, **26**, 2268 (2014).
(38) Y. Xia, K. Sun, and J. Ouyang, *J. Mater. Chem. A*, **3**, 15897 (2015).
(39) C. Yeon, S. J. Yun, J. Kim, and J. W. Lim, *Adv. Electron. Mater.*, **1**, 1500121 (2015).
(40) Y. Zhang, Z. Wu, P. Li, L. K. Ono, Y. Qi, J. Zhou, H. Shen, C. Surya, and Z. Zheng, *Adv. Energy Mater.*, **8**, 1701569 (2018).

(41) G. Giri, D. M. Delongchamp, J. Reinspach, D. A. Fischer, L. J. Richter, J. Xu, S. Benight, A. Ayzner, M. He, and L. Fang, *Chem. Mater.*, **27**, 2350 (2015).
(42) G. Giri, E. Verploegen, S. C. B. Mannsfeld, S. Atahan-Evrenk, D. H. Kim, S. Y. Lee, H. A. Becerril, A. Aspuru-Guzik, M. F. Toney, and Z. Bao, *Nature*, **480**, 504 (2011).
(43) S. Kim, B. Sanyoto, W. Park, S. Kim, S. Mandal, J. Lim, Y. Noh, and J. Kim, *Adv. Mater.*, **28**, 10149 (2016).
(44) U. Voigt, W. Jaeger, G. H. Findenegg, and R. Klitzing, *J. Phys. Chem. B*, **107**, 5273 (2003).
(45) O. Bubnova, Z. U. Khan, H. Wang, S. Braun, D. R. Evans, M. Fabretto, P. Hojati-talemi, D. Dagnelund, J. Arlin, Y. H. Geerts, S. Desbief, D. W. Breiby, J. W. Andereasen, R. Lazzaroni, W. M. Chen, I. Zozoulenko, M. Fahlman, P. J. Murphy, M. Berggren, and X. Crispin, *Nat. Mater.*, **13**, 190 (2013).
(46) T. Lee and Y. Chung, *Adv. Funct. Mater.*, **18**, 2246 (2008).
(47) B. K. Fehse, K. Walzer, K. Leo, W. Lövenich, and A. Elschner, *Adv. Mater.*, **19**, 441 (2007).
(48) B. S. Na, S. Kim, J. Jo, and D. Kim, *Adv. Mater.*, **20**, 4061 (2008).
(49) M.-H. Park, S.-H. Jeong, H.-Y. Seo, C. Wolf, Y.-H. Kim, H. Kim, J. Byun, J. Sung, H. Cho, and T.-W. Lee, *Nano Energy*, **42**, 157 (2017).

